

Accurate modeling of copper precipitation kinetics including Fermi level dependence

Hsiu-Wu Guo^{a)} and Scott T. Dunham

Electrical Engineering Department, University of Washington, Seattle, Washington 98195

(Received 28 July 2006; accepted 17 September 2006; published online 31 October 2006)

Copper is one of the most important contaminants for silicon electronics, and it has detrimental effects on device performance if present in active regions. In this work, the authors investigate copper precipitation models including Fermi level dependence that provide the foundation for simulating copper diffusion and precipitation processes in silicon. These models are verified by comparison to experimental measurements. © 2006 American Institute of Physics.

[DOI: 10.1063/1.2374689]

Copper contamination is of particular concern for silicon electronics due to detrimental effects on lifetime and dielectric reliability, combined with fast diffusivity down to room temperature. The low solubility of copper near room temperature¹ means that precipitation kinetics play an important role in contamination. Unusual precipitation behavior of copper after rapid quenching has been reported by Flink *et al.*^{2,3} (see Fig. 1), where the remaining interstitial Cu concentration equals the initial concentration at relatively low Cu concentration, reaches a maximum, and then starts to drop beyond a critical level which depends on the dopant concentration. These results suggest a strong Fermi level dependence for copper precipitation.

Three major mechanisms are considered for copper redistribution in silicon: pairing, diffusion, and precipitation. Positively charged copper (Cu^+) pairs with acceptors (e.g., B^-) in bulk regions.^{4,5} Copper diffuses interstitially with rapid redistribution at room temperature. Precipitation kinetics involves nucleation and growth. We capture this behavior by considering the evolution of precipitate size density. The resulting model is characterized with experimental data of Flink *et al.* and demonstrates the effectiveness for modeling copper behavior in silicon.

It is believed that the dominant form of copper in silicon is as an interstitial species acting as a single donor (Cu^+).⁴ Positively charged copper also pairs with acceptors such as boron.⁵ Experimental studies of copper-acceptor dissociation energy reported by Wagner *et al.*⁶ show that the dissociation energy varies with different acceptors and is 0.61 eV for CuB. The Fermi level depends on boron and copper concentrations and can be derived from mass action and charge neutrality.

Numerous models have been previously developed to study precipitation process. Both Tsai *et al.*⁷ and Orlowski *et al.*⁸ have used classic simple precipitation model by considering a single fixed cluster, which qualitatively describes precipitation behavior. However, these models are not sufficient to capture the effects of thermal history resulting from various thermal cycles in very large scale integration fabrication process, as the behavior of precipitates is a strong function of size and shape, which depends on the thermal history of the sample. In order to capture this behavior, the kinetic precipitation model has been developed,⁹ which con-

siders the evolution of the precipitate size distribution based on solute concentration and temperature.

To understand the driving force needed for precipitation, the free energy needs to be calculated. Precipitates only form when the concentration of free copper is above a certain level (solubility) so that forming a separate dopant-rich phase reduces the free energy. However, there is an energy barrier which must be overcome at a finite precipitate size due to surface and strain energy. The free energy change upon precipitate formation can be written as

$$\Delta G_n = -nkT \ln \left(\frac{C_{\text{Cu}}}{C_{\text{ss}}} \right) + \Delta G_n^{\text{excess}}, \quad (1)$$

where n is the size of the precipitate and C_{Cu} is the concentration of solute. The excess energy ($\Delta G_n^{\text{excess}}$) becomes proportional to the precipitate surface area for large sizes.⁹

Two important factors regarding the free energy calculated in Eq. (1) must be considered: charge and strain. Weber *et al.*¹ reported that positive-charged (Cu^+) copper is dominant in silicon, while copper precipitates must be nearly neutral, due to Coulombic repulsion. A huge volume change is involved in copper precipitation process; $V_{\text{Cu}_3\text{Si}} \approx 2.3V_{\text{Si}}$. Thus for three-dimensional (3D) precipitates (e.g., spherical), precipitation must either incorporate vacancies (V) and/or eject interstitials (I). However, at low temperatures, self-diffusion is very slow [activation energy of 4–5 eV (Ref. 10)]. Thus, the formation of 3D precipitates is possible only near point defect sinks/sources (e.g., surface, stacking faults, dislocation loops, voids). Since homogeneous nucleation cannot satisfy free volume at low temperatures, stress is minimized via formation of flat disk-shaped precipitates.¹¹ Since planar defects do not require point defect incorporation, the effective solubility is then independent of point defect concentrations, depending only on Fermi level.

$$C_{\text{ss}}^{\text{eff}} = C_{\text{ss}}^{i,\text{disk}} \left(\frac{P}{n_i} \right). \quad (2)$$

The intrinsic solubility associated with planar defects ($C_{\text{ss}}^{i,\text{disk}}$) is higher than for volume precipitates, but this is more than compensated by the elimination of requirements for point defect incorporation.

For disk-shaped defects, the free energy can be written as¹²

^{a)}Electronic mail: hwg@u.washington.edu

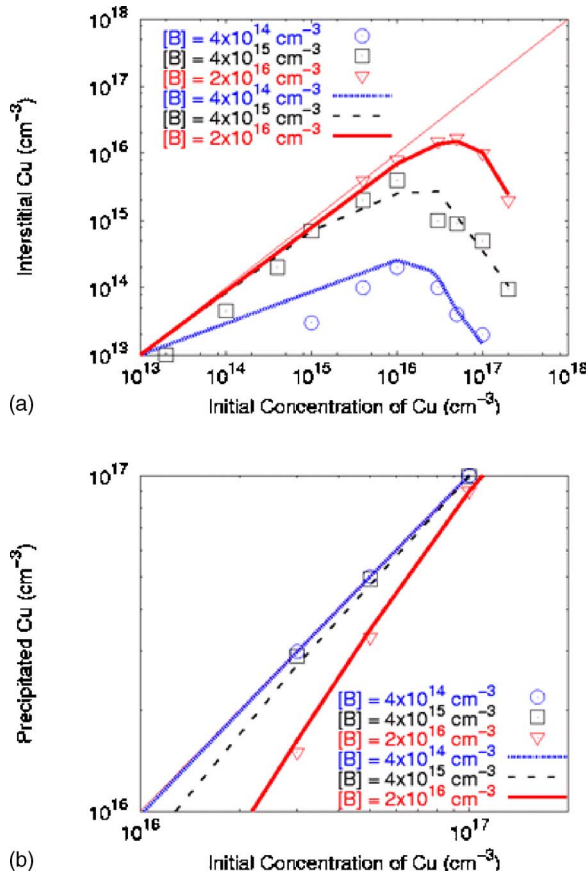


FIG. 1. (Color online) (a) Interstitial copper concentration as measured with transient ion drift of 30 min after quench to room temperature vs initial copper concentration at in-diffusion temperature in three samples with different dopant concentrations ($C_B = 4 \times 10^{14}$, 4×10^{15} , and 2×10^{16} cm⁻³). (b) Precipitated copper concentration measured with x-ray fluorescence vs initial copper concentration at in-diffusion temperature. Points are the experimental data from Flink *et al.* (Refs. 2 and 3) and lines are simulation results.

$$\Delta G_n = -nkT \ln\left(\frac{C_{Cu}}{C_{ss}^{eff}}\right) + (2\pi R_n)\gamma, \quad (3)$$

where γ (eV/cm) is the surface/strain energy per unit perimeter, and R_n is the radius of the disk. Assuming the total volume of disk-shaped precipitate is equal to the product of the number of the solute atoms and its unit volume ($n\Omega = \pi R_n^2 d$), we then get

$$R_n = \sqrt{\frac{n\Omega}{\pi d}}, \quad (4)$$

where Ω is the volume density and d is the thickness of the disk. Figure 2 shows Eq. (3) for three different supersaturation ratios (C_{Cu}/C_{ss}^{eff}). As can be seen, there is a peak value or nucleation barrier, which can be expressed as

$$\Delta G_{n_c} = \frac{\gamma^2 \pi \Omega}{dkT[\ln(C_{Cu}/C_{ss}^{eff}) - \ln(p/n_i)]}. \quad (5)$$

Since the rate of nucleation depends on the exponential of the nucleation barrier [Eq. (5)], as the material changes from n type to p type the nucleation barrier rises strongly and nucleation shuts off abruptly.

To determine the effects of the previous thermal history on precipitation process, we keep track of the time evolution of full precipitate size distribution.⁹ The time evolution of precipitate density can be described by rate equations:

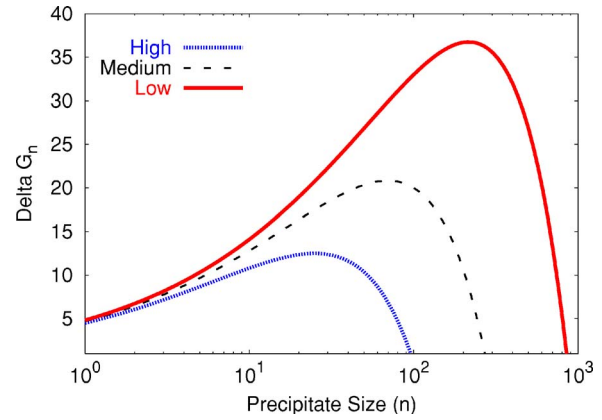


FIG. 2. (Color online) Example plot of free energy vs precipitate size with three different supersaturation ratios (C_{Cu}/C_{ss}^{eff} , high, medium, and low). Notice that these different ratios could be due to the changes in solute, point defect, or carrier (Fermi level) concentrations as indicated in Eq. (2).

$$\frac{df_n}{dt} = I_{n-1} - I_n, \quad n \geq 2, \quad (6)$$

where I_n is the growth rate from size n to $n+1$, and f_n is the concentration of cluster size n . An additional term must be calculated to keep track of solute atoms, since they are involved in the growth of precipitates of all sizes.

$$\frac{dC_{Cu}}{dt} = \frac{df_1}{dt} = -2I_1 - \sum_{n=2}^{\infty} I_n. \quad (7)$$

The flux in precipitate size space from size n to $n+1$ is given by the difference between the growth rate of size n and the dissolution rate of size $n+1$:

$$I_n = D_{Cu} \lambda_n (C_{Cu} f_n - C_n^* f_{n+1}), \quad (8)$$

where λ_n is the kinetic factor associated with the shape of precipitate and diffusivity of solute. $C_{Cu} \approx C_{Cu^+}$ is the solute concentration. C_n^* is defined such that in equilibrium there is no energy difference with the transition from size n to size $n+1$ [$\Delta G_{n+1} = \Delta G_n$ in Eq. (1)].

$$C_n^* = C_{ss}^{eff} \exp\left(\frac{\Delta G_{n+1}^{excess} - \Delta G_n^{excess}}{kT}\right). \quad (9)$$

The kinetic growth factor (λ_n) can be calculated by considering steady-state diffusion in neighborhood of growing precipitate. For spherical precipitates, it is just A_n/R_n . For disk-shaped defects, the kinetic growth factor (λ_n) can be derived as^{9,12}

$$\lambda_n = \frac{A_n}{R_n^{eff} + D_{Cu}/k_n}, \quad (10)$$

where $R_n^{eff} = b \ln(8R_n/b)$, $A_n = 4\pi^2 R_n b$, b is the reaction distance, and k_n is the interface reaction rate.

As for other metal-semiconductor interfaces, we assume that a high density of interface states pins the Fermi level (E_{Fp}) at precipitate surface. This does not change the energetics, since charge transfer is already included, but it does affect the kinetics due to a built-in electric field, which reduces the concentration of Cu^+ near the periphery of precipitate in p -type material. Thus, copper precipitation slows down when the material is more p type. This effect can be included in kinetic factor. Applying Eq. (4) with $b=d=\Omega^{1/3}$,

$$\lambda_n = \frac{4\pi^{1.5}d\sqrt{n}}{0.5 \ln(n) + \ln(8/\sqrt{\pi}) + (p/p_{\text{ref}})}, \quad (11)$$

where

$$p_{\text{ref}} = n_i \exp\left(\frac{E_i - E_{Fp}}{kT}\right) \quad (12)$$

is the hole concentration at the precipitate surface.

The approach described above in which the full set of discrete rate equations [Eq. (6)] is solved accurately captures the size evolution, but it requires a large calculation. To reduce the number of equations and increase the time efficiency, the system can be assumed to be nearly continuous for large precipitate sizes with the use of Fokker-Planck equation^{13,14} and then the size distribution rediscritized more coarsely. Figure 1(a) shows the comparison between experimental data and simulation results for remaining interstitial copper concentration versus the initial copper concentration. The simulation results agree very well with experimental data and predict the peak value for different C_B . For initial copper concentration less than the boron concentration, almost no precipitation occurs even though the concentration is well above room temperature solubility. The main reason for this phenomenon is dependence of solubility and thus nucleation barrier on Fermi level. Also, due to that fact the Fermi level is pinned at the interface, it causes a built-in electric field, repelling Cu^+ near the periphery of the precipitate more significantly in strongly p -type material ($C_B = 2 \times 10^{16} \text{ cm}^{-3}$). For higher initial copper concentration, the copper precipitation process continues dropping the interstitial copper well below the boron concentration since critical nuclei already exist.

Figure 1(b) shows the comparison between experimental data and simulation results for precipitated copper concentration versus initial copper concentration. Again the model does an excellent job of capturing behavior. For high dopant concentration ($C_B = 2 \times 10^{16} \text{ cm}^{-3}$), solute tends to outdiffuse instead of precipitating in the bulk, due to increased nucleation barrier in p -type material.

This work has addressed the modeling of copper precipitation in silicon. Building on previous related efforts, new models were developed to simulate the precipitation processes, based on evolution of size distribution and charge of solute and precipitate. The nucleation barrier depends strongly on the supersaturation and thus the solubility, which leads to strong Fermi level effects due to dominant positive charge state of interstitial copper. Once the nucleation barrier is overcome, precipitate will keep growing as long as the solute concentration is above the solubility. We have demonstrated that models can predict the behavior of the copper precipitation for low thermal budget process, where the precipitates are platelike, by comparing the simulation results to the experimental findings reported by Flink *et al.*^{2,3}

This work was supported by SiWEDS (Silicon Wafer Engineering and Defect Science) a NSF Industry/University Cooperative Research Center.

- ¹E. Weber, Appl. Phys. A: Solids Surf. **30**, 1 (1983).
- ²A. Istratov, C. Flink, H. Hieslmair, S. McHugo, and E. Weber, Mater. Sci. Eng., B **72**, 99 (2000).
- ³C. Flink, H. Feick, S. McHugo, W. Seifert, H. Hieslmair, T. Heiser, A. Istratov, and E. Weber, Phys. Rev. Lett. **85**, 4900 (2000).
- ⁴R. Hall and J. Racette, J. Appl. Phys. **35**, 379 (1964).
- ⁵R. L. Meek and T. Seidel, J. Phys. Chem. Solids **36**, 731 (1975).
- ⁶P. Wagner, H. Hage, H. Prigge, T. Prescha, and J. Weber, in *Proceedings of the Sixth International Symposium on Silicon Materials Science and Technology: Semiconductor Silicon 1990*, edited by H. Huff, K. Barraclough, and J. I. Chikawa (Electrochemical Society, Pennington, NJ, 1990), p. 675.
- ⁷M. Y. Tsai, F. Morehead, J. Baglin, and A. Michel, J. Appl. Phys. **51**, 3230 (1980).
- ⁸M. Orłowski, R. Subrahmanyam, and G. Huffman, J. Appl. Phys. **71**, 164 (1992).
- ⁹S. T. Dunham, J. Electrochem. Soc. **142**, 2823 (1995).
- ¹⁰J. Plummer, M. Deal, and P. Griffin, *Silicon VLSI Technology* (Prentice-Hall, Upper Saddle River, NJ, 2000).
- ¹¹M. Seibt, M. Griess, A. Istratov, H. Hedemann, A. Sattler, and W. Schroeter, Phys. Status Solidi A **171**, 166 (1998).
- ¹²S. T. Dunham, Appl. Phys. Lett. **63**, 464 (1993).
- ¹³L. Demeio and B. Shizgal, J. Chem. Phys. **98**, 5713 (1993).
- ¹⁴C. F. Clement and M. Wood, Proc. R. Soc. London, Ser. A **371**, 553 (1980).